JOURNAL OF TISSUE ENGINEERING AND REGENERATIVE MEDICINE
J Tissue Eng Regen Med 2008; **2**: 445–449.
Published online in Wiley InterScience (www.interscience.wiley.com) **DOI:** 10.1002/term.111

SHORT COMMUNICATION

Human adipose tissue-derived mesenchymal stem cells as a novel feeder layer for epithelial cells

Hiroaki Sugiyama[1], Kazuhisa Maeda[2,3], Masayuki Yamato[4], Ryuhei Hayashi[1], Takeshi Soma[1], Yasutaka Hayashida[1], Joseph Yang[4], Masayuki Shirakabe[3], Akifumi Matsuyama[3], Akihiko Kikuchi[4], Yoshiki Sawa[3], Teruo Okano[4], Yasuo Tano[1] and Kohji Nishida[1,5]*

[1]*Department of Ophthalmology, Osaka University Medical School, Osaka 565-0871, Japan*
[2]*Department of Metabolic Medicine and Molecular Science, Osaka University Medical School, Osaka 565-0871, Japan*
[3]*Medical Centre for Translational Research, Osaka University Hospital, Osaka 565-0871, Japan*
[4]*Institute of Advanced Biomedical Engineering and Science, Tokyo Women's Medical University, TWIns, Tokyo 162-8666, Japan*
[5]*Department of Ophthalmology and Visual Science, Tohoku University Graduate School of Medicine, Sendai 980-8574, Japan*

Abstract

We examined a novel human feeder cell layer of mesenchymal stem cells harvested from human adipose tissues. Gene expression analyses and colony-forming assay with human primary epithelial cells showed that the adipose tissue-derived mesenchymal stem cells produced various factors to support epithelial stem/progenitor maintenance and cell growth. Using the mesenchymal stem cells as novel feeder layers, transplantable epithelial cell sheets could be effectively generated *ex vivo* on temperature-responsive cell-culture surfaces. Copyright © 2008 John Wiley & Sons, Ltd.

Received 11 June 2008; Accepted 12 June 2008

Keywords **mesenchymal stem cell; cornea; oral mucosa; skin; stem cell; 3T3 cell, epithelium**

1. Introduction

Since 1975, murine 3T3 feeder layer cells have been utilized for the *in vitro* expansion of various epithelial cell types, including epidermal cells (Rheinwald *et al.*, 1975), corneal epithelial cells (Pellegrini *et al.*, 1997) and urothelial cells (Schaefer *et al.*, 1998). Additionally, since 1981, autologous epidermal cells expanded using the 3T3 feeder layer method have been used to treat severe burns patients (Gallico *et al.*, 1984). Similarly, several groups, including ours, have initiated early clinical trials using cultured corneal epithelial cells (Pellegrini *et al.*, 1997) and oral mucosal epithelial cells (Nishida *et al.*, 2004b; De Luca *et al.*, 2006) for various other applications, such as corneal surface reconstruction. However, with the use of expanded epithelial cells, a major shortcoming is the use of mouse-derived 3T3 feeder layers that are required for the *in vitro* maintenance and propagation of epithelial stem cells. Although epidermal cell culture services in Good Manufacturing Practice (GMP) facilities have been commercially available in the USA since 1988, tissues created using murine 3T3 cells are classified by the US Food and Drug Administration (FDA) as xenografts, which hinder their widespread use. Another drawback of the conventional culture conditions for epithelial cells is the use of fetal bovine serum (FBS). Human embryonic stem cells cultured using animal-derived feeder layers and serum are also known to incorporate immunogenic, non-human sialic acids (Martin *et al.*, 2005), further emphasizing the need to eliminate the need for mouse 3T3 cells and FBS. In the present study, we present the development of a novel human feeder layer composed of adipose-derived mesenchymal stem cells that can eliminate the need for animal-derived products in epithelial cell cultures.

2. Materials and methods

This study was approved by the institutional review board of Osaka University Medical School, Japan.

Correspondence to: Kohji Nishida, Department of Ophthalmology and Visual Science, Tohoku University Graduate School of Medicine, 1-1 Seiryo-machi, Aoba-ku, Sendai, Miyagi, 980-8574, Japan. E-mail: knishida@oph.med.tohoku.ac.jp

2.1. Cell culture

Adipose-derived mesenchymal stem cells were isolated as described previously (Miyahara *et al.*, 2006). For colony-forming assays, human limbal epithelial cells were isolated from cadaveric donor corneas (Northwest Lions Eye Bank, Seattle, WA, USA). Oral mucosal epithelial cells and skin epidermal cells were isolated from tissues provided by volunteer donors. Human serum was also obtained from the same donors who provided the adipose-derived mesenchymal stem cells. To make feeder layers, human adipose-derived mesenchymal stem cells and NIH/3T3 cells were lethally irradiated (20 Gy X-rays) and seeded onto commercially available culture dishes (BD Biosciences, Franklin Lakes, NJ, USA). For colony-forming assays, epithelial cells were cultured using the feeder layer method in keratinocyte culture medium (Rheinwald *et al.*, 1975) containing 5% human serum or FBS. After 10–14 days, the dishes were fixed and stained with rhodamine B. All assays were run in duplicate for five independent samples. Using temperature-responsive culture inserts (CellSeed Inc., Tokyo, Japan), carrier-free transplantable epithelial cell sheets were prepared according to specific procedures described previously (Nishida *et al.*, 2004a, 2004b), with the replacement of 3T3 feeder cells and FBS, by human mesenchymal stem cells and human serum, respectively. For immunofluorescence, harvested human epithelial cell sheets were embedded in OCT compound and processed into 10 μm frozen tissue sections. After drying for 1 h at room temperature, the tissue sections were washed with Tris-buffered saline (TBS, Takara Bio, Shiga, Japan) three times, and incubated with TBS containing 5% donkey serum and 0.3% Triton X for 1 h to block non-specific reactions. The sections were then incubated with a 1:200 dilution of anti-keratin 1 (K1; LHK1, Abcam, Cambridge, UK), anti-keratin 10 (K10; DE-K10, DakoCytomation, Glostrup, Denmark), anti-keratin 14 (K14; LL001, Abcam), anti-keratin 15 (K15; LHK15, Chemicon, Temecula, CA), anti-p63 (4A4; Santa Cruz Biotechnology, Santa Cruz, CA, USA) or anti-Muc16 (Ov185; Abcam) antibodies at 4 °C overnight. The slides were again washed twice with TBS, and incubated with a 1:200 dilution of Alexa-Fluor® 488-conjugated secondary antibodies (Molecular Probes, Eugene, OR, USA). All tissue sections were finally counterstained with propidium iodide (Sigma, St. Louis, MO, USA) and observed by fluorescence microscopy (Axiovert 200, Carl Zeiss, Jena, Germany).

2.2. RT–PCR

Total RNA was obtained from lethally irradiated human adipose-derived mesenchymal stem cells and murine NIH/3T3 cells using the RNeasy total RNA kit (Qiagen, Valencia, CA, USA). Reverse transcription was performed with the SuperScript First-Strand Synthesis System for RT-PCR (Invitrogen, Carlsbad, CA, USA). Forward (-F) and reverse (-R) primer sets for human (h) and mouse (m) pleiotrophin (PTN), epiregulin (EPR), cystatin C (CC), hepatocyte growth factor (HGF), keratinocyte growth factor (KGF), sonic hedgehog (Shh), insulin-like growth factor 1a (IGF1a) and glyceraldehyde-3-phosphate dehydrogenase (GAPDH) were as follows. *hPTN-F*, AGAGGACGTTTCCAACTCAA; *hPTN-R*, TATGTTCCACAGGTGACATC; *hEPR-F*, AGGAGGATGGAGATGCTCTG; *hEPR-R*, TCAGACTTGCGGCAACTCTG; *hCC-F*, TCCTCTCTATCTAGCTCCAG; *hCC-R*, TCCTGACAGGTGGATTTCGA; *hHGF-F*, GCCTGAAAGATATCCCGACA; *hHGF-R*, TTCCATGTTCTTGTCCCACA; *hKGF-F*, GGAGGAATCCTGTGTTGTTA; *hKGF-R*, CTAAGGTTCATGAGCAGTAC; *hShh-F*, CGGAGCGAGGAAGGGAAAG; *hShh-R*, TTGGGGATAAACTGCTTGTAGGC; *hIGF1a-F*, ATGCACACCATGTCCTC; *hIGF1a-R*, CATCCTGTAGTTCTTGTTTC; *hGAPDH-F*, ACCACAGTCCATGCCATCAC; *hGAPDH-R*, TCCACCACCCTGTTGCTGTA; *mPTN-F*, GGACCTCTGCAAGCCAAAAAA; *mPTN-R*, GCACTCAGCTCCAAACTGCTTC; *mEPR-F*, AGCTGCACCGAGAAAGAAGGA; *mEPR-R*, AGAAGTGCTCACATCGCAGACC; *mCC-F*, AGCTCGTGGCTGGAGTGAACTA; *mCC-R*, CCTGCAGCAGCTCCTTTACTGT; *mHGF-F*, GGTGAAAGCTACAGAGGTCCCA; *mHGF-R*, ATGGTATTGCTGGTTCCCCTG; *mKGF-F*, GAGTTTAAGCAGGAGCATCGCA; *mKGF-R*, CGTTCTTTTCCACGTGCTTGAT; *mShh-F*, CCCAAAAAGCTGACCCCTTTAG; *mShh-R*, TCCACTGCTCGACCCTCATAGT; *mIGF1a-F*, TATGGCTCCAGCATTCGGA; *mIGF1a-R*, GCGGTGATGTGGCATTTTCT; *mGAPDH-F*, ATCACTGCCACCCAGAAGACTG; and *mGAPDH-R*, TGCTGTTGAAGTCGCAGGAGA. Thermocycling programmes consisted of an initial step at 94 °C for 5 min and 35 cycles at 94 °C for 30 s, 58 °C for 30 s and 72 °C for 30 s, followed by a final step at 72 °C for 7 min. Negative controls using non-reverse transcribed total RNA as template strands were performed for all experiments. All assays were run in duplicate.

3. Results and discussion

The morphology of human mesenchymal stem cells (Figure 1A) was similar to that of NIH/3T3 cells (Figure 1B). The mesenchymal stem cells and NIH/3T3 cells also both expressed various genes that have been previously shown to maintain epithelial stem/progenitor cells and/or promote proliferation of epithelial cells, including PTN (Mitsiadis *et al.*, 1995), EPR (Shirakata *et al.*, 2000), CC (Taupin *et al.*, 2000), HGF (Rubin *et al.*, 1989), KGF (Finch *et al.*, 1989) and IGF1a (Tavakkol *et al.*, 1992) (Figure 1C). Although Shh has been reported to promote proliferation of epithelial cells (Kameda *et al.*, 2001), its expression was not detected in either feeder cell type. Colony-forming assay with three types of human primary epithelial cells, limbal epithelial cells, oral mucosal epithelial cells, and skin epidermal cells revealed that human mesenchymal stem cells had the ability to support epithelial cell growth, similar to conventional

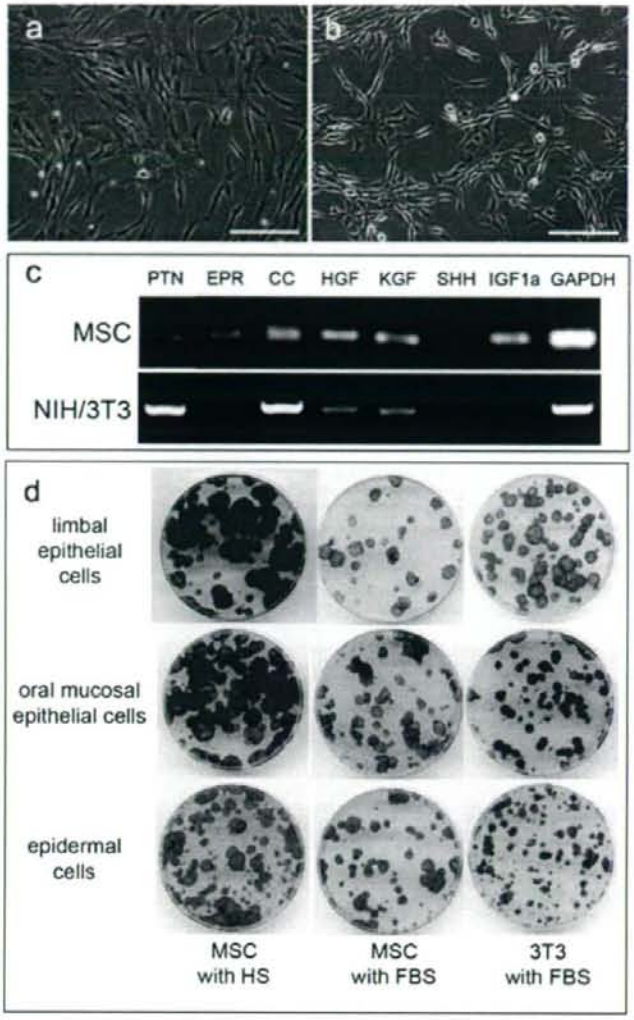

Figure 1. Feeder layers. Adipose-derived mesenchymal stem cells (a; MSC in c, d) and NIH/3T3 cells (b) were examined by phase-contrast microcopy, RT–PCR (c) and colony-forming assay (d)

3T3 feeder layers (Figure 1D). In comparison to 3T3 feeder layers, the mesenchymal stem cells had slightly decreased colony-forming efficiencies; however, we found that the use of autologous human serum was more effective than FBS at maintaining these colony-forming cells, when used with the mesenchymal stem cell feeder layers. Additionally, the mesenchymal stem cell feeder layers produced larger colonies with smooth perimeters, a property specific to epithelial stem/progenitor cells (Barrandon *et al.*, 1987) when cultured with human serum. From our previous clinical successes in corneal surface reconstruction (Nishida *et al.*, 2004a, 2004b), we fabricated transplantable corneal and oral mucosal epithelial cell sheets using the human mesenchymal stem cell feeder layers and human serum (Figure 2). Cell sheets, harvested from temperature-responsive culture surfaces by temperature reduction to 20 °C, consisted of three to five cell layers resembling the native corneal epithelium. Immunofluorescence analyses revealed that cell sheets created using both feeder layers showed similar expression of various epithelial cell markers. p63, a putative stem/progenitor cell marker (Pellegrini *et al.*, 2001), was positive in the basal cells of the stratified epithelial cell sheets. K15, another putative epithelial stem/progenitor marker (Webb *et al.*, 2004), was also positive in the basal cells. K14,which is expressed in the basal and suprabasal cells of the corneal and skin epithelia (Yoshida *et al.*, 2006), was positive in almost all layers of the harvested cell sheets. K1 and K10, specifically expressed in the stratum corneum of the keratinized

DOI: 10.1002/term

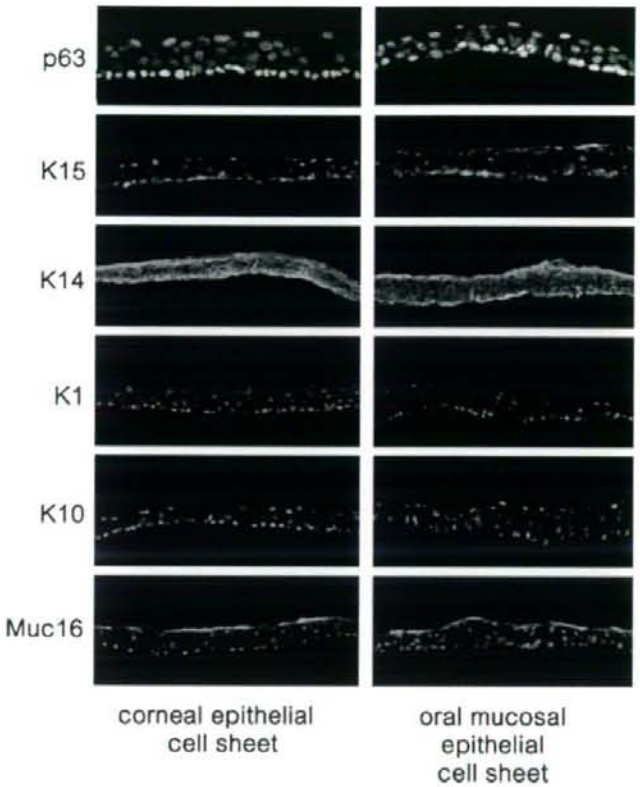

Figure 2. Immunofluorescence of transplantable human epithelial cell sheets. Nuclei are stained with propidium iodide (red) in all panels

epidermis (Gu *et al.*, 2007), were both negative in all cells of the harvested cell sheets. Muc16, a membrane-associated mucin present in the cells of the ocular surface epithelium (Argueso *et al.*, 2003), was also expressed by the superficial cells of the cell sheets. These results showed that the use of the human mesenchymal stem cells and human serum was able to generate transplantable epithelial cell sheets, similar to conventional methods using NIH/3T3 feeder layers and FBS. Since adipose tissues are isolated via procedures that are commonly used in plastic and reconstructive surgeries, our results present the development of a novel and capable autologous feeder layer from a readily available source for epithelial regenerative medicine.

Acknowledgements

Supported by the High-Tech Research Centre Programme and the Formation of Innovation Centre for Fusion of Advanced Technologies in the Special Coordination Funds for Promoting Science and Technology, from the Ministry of Education, Culture, Sports, Science and Technology (MEXT), Japan, and the Suzuken Memorial Foundation.

References

Argueso P, Spurr-Michaud S, Russo CL, *et al.* 2003; MUC16 mucin is expressed by the human ocular surface epithelia and carries the H185 carbohydrate epitope. *Invest Ophthalmol Vis Sci* **44**: 2487–2495.

Barrandon Y, Green H. 1987; Three clonal types of keratinocyte with different capacities for multiplication. *Proc Natl Acad Sci USA* **84**: 2302–2306.

De Luca M, Pellegrini G, Green H. 2006; Regeneration of squamous epithelia from stem cells of cultured grafts. *Regen Med* **1**: 45–57.

Finch PW, Rubin JS, Miki T, *et al.* 1989; Human KGF is FGF-related with properties of a paracrine effector of epithelial cell growth. *Science* **245**: 752–755.

Gallico GG III, O'Connor NE, Compton CC, *et al.* 1984; Permanent coverage of large burn wounds with autologous cultured human epithelium. *N Engl J Med* **311**: 448–451.

Gu LH, Coulombe PA. 2007; Keratin function in skin epithelia: a broadening palette with surprising shades. *Curr Opin Cell Biol* **19**: 13–23.

Kameda T, Hatakeyama S, Terada K, *et al.* 2001; Acceleration of the formation of cultured epithelium using the sonic hedgehog expressing feeder cells. *Tissue Eng* **7**: 545–555.

Martin MJ, Muotri A, Gage F, *et al.* 2005; Human embryonic stem cells express an immunogenic non-human sialic acid. *Nat Med* **11**: 228–232.

Mitsiadis TA, Salmivirta M, Muramatsu T, *et al.* 1995; Expression of the heparin-binding cytokines, midkine (MK) and HB-GAM (pleiotrophin) is associated with epithelial–mesenchymal interactions during fetal development and organogenesis. *Development* **121**: 37–51.

Miyahara Y, Nagaya N, Kataoka M, *et al.* 2006; Monolayered mesenchymal stem cells repair scarred myocardium after myocardial infarction. *Nat Med* **12**: 459–465.
Nishida K, Yamato M, Hayashida Y, *et al.* 2004a; Functional bioengineered corneal epithelial sheet grafts from corneal stem cells expanded *ex vivo* on a temperature-responsive cell culture surface. *Transplantation* **77**: 379–385.
Nishida K, Yamato M, Hayashida Y, *et al.* 2004b; Corneal reconstruction with tissue-engineered cell sheets composed of autologous oral mucosal epithelium. *N Engl J Med* **351**: 1187–1196.
Pellegrini G, Dellambra E, Golisano O, *et al.* 2001; p63 identifies keratinocyte stem cells. *Proc Natl Acad Sci USA* **98**: 3156–3161.
Pellegrini G, Traverso CE, Franzi AT, *et al.* 1997; Long-term restoration of damaged corneal surfaces with autologous cultivated corneal epithelium. *Lancet* **349**: 990–993.
Rheinwald JG, Green H. 1975; Serial cultivation of strains of human epidermal keratinocytes: the formation of keratinizing colonies from single cells. *Cell* **6**: 331–343.
Rubin JS, Osada H, Finch PW, *et al.* 1989; Purification and characterization of a newly identified growth factor specific for epithelial cells. *Proc Natl Acad Sci USA* **86**: 802–806.
Schaefer BM, Lorenz C, Back W, *et al.* 1998; Autologous transplantation of urothelium into demucosalized gastrointestinal segments: evidence for epithelialization and differentiation of *in vitro* expanded and transplanted urothelial cells. *J Urol* **159**: 284–290.
Shirakata Y, Komurasaki T, Toyoda H, *et al.* 2000; Epiregulin, a novel member of the epidermal growth factor family, is an autocrine growth factor in normal human keratinocytes. *J Biol Chem* **275**: 5748–5753.
Taupin P, Ray J, Fischer WH, *et al.* 2000; FGF-2-responsive neural stem cell proliferation requires CCg, a novel autocrine/paracrine cofactor. *Neuron* **28**: 385–397.
Tavakkol A, Elder JT, Griffiths CE, *et al.* 1992; Expression of growth hormone receptor, insulin-like growth factor 1 (IGF-1) and IGF-1 receptor mRNA and proteins in human skin. *J Invest Dermatol* **99**: 343–349.
Webb A, Li A, Kaur P. 2004; Location and phenotype of human adult keratinocyte stem cells of the skin. *Differentiation* **72**: 387–395.
Yoshida S, Shimmura S, Kawakita T, *et al.* 2006; Cytokeratin 15 can be used to identify the limbal phenotype in normal and diseased ocular surfaces. *Invest Ophthalmol Vis Sci* **47**: 4780–4786.

Experimental Eye Research 87 (2008) 191–196

Contents lists available at ScienceDirect

Experimental Eye Research

journal homepage: www.elsevier.com/locate/yexer

Differential expression of MUC16 in human oral mucosal epithelium and cultivated epithelial sheets

Y. Hori [a,*], K. Nishida [b], M. Yamato [c], H. Sugiyama [a], T. Soma [a], T. Inoue [a], N. Maeda [a], T. Okano [c], Y. Tano [a]

[a] Department of Ophthalmology, Osaka University Medical School, 2-2 Yamadaoka, Room E7, Suita, Osaka 565-0871, Japan
[b] Department of Ophthalmology, Tohoku University Graduate School of Medicine, Sendai, Japan
[c] Institute of Advanced Biomedical Engineering and Science, Tokyo Women's Medical University, Tokyo, Japan

ARTICLE INFO

Article history:
Received 11 December 2007
Accepted in revised form 22 May 2008
Available online 21 July 2008

Keywords:
MUC16
oral mucosal epithelium
cultivated epithelial sheet transplantation
membrane-associated mucin
temperature-responsive culture dish

ABSTRACT

Cultivated oral mucosal epithelial sheet transplantation is a new surgical strategy to treat severe ocular surface disorders such as chemical burns, ocular cicatricial pemphigoid, and Stevens–Johnson syndrome. MUC16 is thought to be the most important membrane-associated mucin on the ocular surface because it forms a protective barrier on the epithelial cell surface. In this study, we studied MUC16 expression in mRNA and protein levels and compared the expression patterns between cultivated oral mucosal epithelial cell sheet and oral mucosal tissue. Specimens (5 × 5 mm) of oral mucosal tissue harvested from healthy volunteers were used. The oral mucosal epithelial cells were cultured on temperature-responsive culture dishes to generate stratified cell sheets. Cultivated oral mucosal epithelial cells formed three- to five-cell thick stratified sheets for 2 weeks. Scanning electron micrographs revealed that the apical surfaces of the oral mucosal tissue and the oral mucosal sheets were covered with dense microvilli/microplicae. Real-time PCR showed significantly more MUC16 transcripts in the cultivated oral mucosal sheets and corneal epithelial sheets than in the oral mucosal tissue ($P = 0.023$ and 0.008, respectively, Mann–Whitney rank sum test). These findings were confirmed by immunohistochemical examination using an MUC16 antibody to the protein. MUC16 protein was localized to the apical cells of the oral mucosal sheets, but the human oral mucosal tissue did not express MUC16 protein in any cell layers. In this study, interestingly, the expression of membrane-associated mucin MUC16 differs between human oral mucosal epithelia and cultivated epithelial sheets. MUC16 expressed in the oral mucosal sheets may contribute to ocular surface reconstruction after oral mucosal sheet transplantation.

1. Introduction

Severe ocular surface diseases, such as chemical burns, ocular cicatricial pemphigoid, and Stevens–Johnson syndrome, lead to severe visual complications. These diseases are characterized by limbal corneal stem cell deficiencies that result in conjunctival invasion of the cornea, corneal opacification, neovascularization, chronic inflammation, and conjunctival scarring (Kinoshita et al., 2001; Tseng, 1989). To date, ocular surface reconstruction techniques such as keratoepithelioplasty, limbal transplantation, and amniotic membrane transplantation have been reported to treat these diseases (Kenyon and Tseng, 1989; Tan et al., 1996; Thoft, 1984; Tseng, 1989; Tsubota et al., 1996). Recently, several investigators have reported that cultivated autologous oral mucosal epithelial sheet transplantation is effective for reconstructing the ocular surface in patients with total limbal stem cell deficiencies (Inatomi et al., 2006; Nakamura et al., 2004, 2007; Nishida et al., 2004b).

Cultivated oral mucosal epithelial cells differ from corneal or conjunctival epithelia. For example, surviving transplanted cultivated oral mucosal epithelium on the corneas of patients after oral mucosal epithelial sheet transplantation was reported positive for keratin K3 and K4 and negative for K10 and K12, indicating that it was neither corneal nor conjunctival tissue (Inatomi et al., 2006). Sekiyama et al. (2006) reported that antiangiogenic factors contributing to corneal avascularity, thrombospondin-1, pigment epithelium derived factor (PEDF), and endostatin, were expressed more highly in a cultivated corneal epithelial sheet than in a cultivated oral mucosal epithelial sheet. It is still unclear why the ectopically transplanted oral mucosal epithelial sheet that differs from corneal epithelium can survive successfully on the corneas of patients with ocular surface diseases.

Mucins are large, highly *O*-glycosylated molecules with a high molecular weight that are present at the interface between epithelia with a wet surface and their extracellular environment (Hattrup and Gendler, 2008). On the ocular surface, mucins

* Corresponding author. Tel.: +81 6 6879 3456; fax: +81 6 6879 3458.
E-mail address: hori@ophthal.med.osaka-u.ac.jp (Y. Hori).

0014-4835/$ – see front matter © 2008 Elsevier Ltd. All rights reserved.
doi:10.1016/j.exer.2008.05.014

maintain the healthy and non-keratinized ocular surface by preventing desiccation of the epithelial surface, lubricating the ocular surface during blinking, and providing a barrier to penetration of pathogens (Blalock et al., 2007; Fleiszig et al., 1994; Gipson and Argueso, 2003; Inatomi et al., 1996). Mucins are classified as membrane-associated mucins or secreted mucins. At least three membrane-associated mucins (MUC1, MUC4, and MUC16) and three secreted mucins (MUC5AC, MUC2, and MUC7) are expressed on the ocular surface (Argueso et al., 2003; Gipson, 2004; Inatomi et al., 1995; Jumblatt et al., 2003; McKenzie et al., 2000; Pflugfelder et al., 2000).

In the oral cavity, mucins are providing a mucus barrier with their viscoelastic properties (Kutta et al., 2006) as well as ocular surface. Two well-known secreted mucins, mucus glycoprotein 1 (MG1) and mucus glycoprotein 2 (MG2), have been identified based on chemical composition and molecular weight in the oral cavity. High-molecular-weight MG1 consists mainly of the MUC5B gene product (Nielsen et al., 1997), whereas the low-molecular-weight MG2 is a product of the MUC7 gene (Bobek et al., 1993). However, only a few investigators have reported expression of membrane-associated mucins in the human oral cavity. Sengupta et al. (2001) reported that MUC1 was expressed in the ducts of the minor salivary glands by immunohistochemistry and in situ hybridization. Using reverse transcriptase (RT)–PCR and Northern blotting analysis, Liu et al. (2002) reported that MUC1 and MUC4 but not MUC3 and MUC13 were expressed in the human parotid and submandibular glands but not in the oral mucosal epithelial cells determined. We recently reported preliminary data that indicated that cultivated stratified human oral mucosal epithelial sheet expressed the transcripts for membrane-associated mucins, MUC1, MUC4, and MUC16 but not MUC3, MUC12, MUC13, MUC15, and MUC17, the expression pattern of which was the same as that in ocular surface epithelium (Hori et al., 2007).

MUC16 is a larger molecule than other membrane-associated mucins, i.e., MUC1 and MUC4, on the ocular surface (O'Brien et al., 2002; Yin and Lloyd, 2001). Jager et al. (2007) demonstrated that MUC16 was also present in the all lacrimal apparatus, i.e., lacrimal gland, accessory lacrimal glands, and nasolacrimal ducts. MUC16 expressed on the tips of the microplicae of the ocular surface is a major component of the ocular surface glycocalyx (Argueso et al., 2006). Blalock et al. (2007) showed that siRNA-mediated knockdown of MUC16 on the stratified human corneal epithelial cells increased the penetrance of Rose Bengal dye and adherence of *Staphylococcus aureus* to the corneal epithelial cells. Recently, Paulsen et al. (2008) reported that shedding of MUC16 from the ocular surface was regulated by inflammatory mediators, bacterial components and bacterial supernatants. These data indicate that MUC16 may be the most important membrane-associated mucin on the ocular surface because it forms a protective barrier on the epithelial cell surface.

The purpose of the current study was to investigate the expression of membrane-associated mucins MUC16 in the human oral mucosal epithelial cells. We studied MUC16 expression in mRNA and protein levels and compared the expression patterns between cultivated oral mucosal epithelial cell sheet and oral mucosal tissue.

2. Material and methods

2.1. Sample collection

All samples were obtained in compliance with institutional review board regulations, informed consent regulations, and the tenets of the Declaration of Helsinki. Oral mucosal tissues were obtained from three healthy volunteers as previously described (Nishida et al., 2004b). After each oral cavity was sterilized with topical povidone–iodine, a 5 × 5-mm specimen of oral mucosal tissue was excised from the interior buccal mucosal epithelium under local anesthesia with xylocaine.

2.2. Cell culture

Oral mucosal epithelial cells were collected by removing all epithelial layers after treatment with Dispase II (3 mg/ml, Roche Diagnostics, Indianapolis, IN), at 37 °C for 1 h. The specimens were placed in trypsin and EDTA for 15 min to form single-cell suspensions. Primary cultures of human corneal epithelial cells were established from the periphery of eye bank corneas (Northwestern Lions Eye Bank, Seattle, WA) after keratoplasty. To eliminate the need for cell carriers and allow harvesting of intact cell sheets, we used the temperature-responsive culture dish system, provided by Cell Seed, Inc. (Tokyo, Japan) (Hirose et al., 2000). The detailed cell culture methods to produce the stratified cell sheets have been reported previously (Hayashida et al., 2005; Nishida et al., 2004a,b). Briefly, the oral mucosal epithelial cells or corneal epithelial cells were cultured together with 3T3 feeder cells treated with mitomycin C on temperature-responsive culture dishes in a 3:1 mixture of Dulbecco's modified Eagle's medium (Invitrogen, Carlsbad, CA) and F12 (Invitrogen), supplemented with 10% fetal bovine serum (Invitrogen) for about 2 weeks with the aim of producing stratified cell sheets.

2.3. Total RNA extraction and real-time PCR

After culture, total RNA from the cells was isolated using EZ1 RNA Mini (QIAGEN Inc., Valencia, CA), according to the manufacturer's recommended protocol. Total RNA from the cells was reverse transcribed using the SuperScript First-Strand Synthesis System for RT–PCR (Invitrogen) as previously described (Argueso et al., 2002). The amount of MUC16 mRNA expression was determined in the oral mucosal epithelial cells by real-time PCR using TaqMan Chemistry and the GeneAmp 7900HT Sequence Detection System (Applied Biosystems, Foster City, CA). After reverse transcription of total RNA (1.0 μg) from the samples, PCR amplification was performed with TaqMan Probes. The primers and TaqMan probes used (MUC16 and GAPDH) have been published (Argueso et al., 2002, 2003; Danjo et al., 2000; Hori et al., 2004). Validation experiments were performed to confirm equivalent PCR efficiencies for GAPDH and the target genes. For relative quantitation, we used the delta C_T method (Applied Biosystems) reported previously (Gipson et al., 2003). In the current study, the amount of MUC16 mRNA expression in human conjunctival tissue was used as the calibrator, i.e., set as 1. Sample number was three, and each sample was assayed in triplicate. Because the amount of total RNA obtained from the primary (uncultured) oral mucosal epithelial cells of each sample was small, those of all three samples were mix together for comparison to others.

2.4. Immunohistochemical analysis

Cryosections from cultured cell sheets and oral mucosal tissue were immunostained with monoclonal anti-MUC16 antibody (OC125, DAKO, Carpinteria, CA) and fluorescein isothiocyanate-labeled secondary antibodies (Jackson ImmunoResearch Laboratories Inc., West Grove, PA). Nuclei were costained with propidium iodide (Sigma–Aldrich, St. Louis, MO). Stained cells were observed using confocal laser scanning microscopy (LSM-510, Carl Zeiss).

2.5. Electron microscopy

Oral mucosal tissues and cultivated oral mucosal epithelial sheets were examined by scanning electron microscopy (SEM) as

previously described (Nishida et al., 2004a). The specimens were fixed in 2.5% glutaraldehyde for 2 h, washed with cacodylate buffer, postfixed in 1.0% osmium tetroxide, and then passed through a graded ethanol series (50%, 70%, 80%, 90%, and 100%). The specimens each were immersed twice in hexamethyldisilazane (TAAB Laboratories Equipment Ltd., Aldermaston, UK) for 10 min, air dried, mounted on aluminum stubs, sputter coated with gold, and examined on the H-7000 (Hitachi, Tokyo, Japan).

2.6. Statistical analysis

Statistical comparisons of results obtained by real-time PCR were performed using the Mann–Whitney rank sum test (SigmaStat v.2.03). $P < 0.05$ was considered significant.

3. Results

3.1. Cultivation of oral mucosal epithelial cells

Native oral mucosal epithelial cells were stratified in 10 to 20 cell layers (Fig. 1A). Cultured oral mucosal epithelial cells reached confluence in about 2 weeks, and after a few more days, they formed three- to five-cell thick stratified sheets (Fig. 1B), with morphology similar to that of cultivated corneal epithelial sheets cultured under the same conditions (Fig. 1C). Scanning electron micrographs revealed numerous microvilli and microplicae on the apical surfaces of the cultivated oral mucosal epithelial sheet (Fig. 2A and B) and oral mucosal tissue (Fig 2C).

3.2. MUC16 expression in the oral mucosal epithelial cells

Expression of membrane-associated mucin MUC16 mRNA was determined by real-time PCR in native oral mucosal epithelial cells and cultivated oral mucosal and corneal epithelial sheets. Expressing all mRNA levels relative to the MUC16 level in the native conjunctival tissue allowed convenient comparisons of the relative amounts of MUC16 expressed in native (uncultured) oral mucosal epithelial cells and cultivated oral mucosal and corneal epithelial sheets. The cultivated oral mucosal epithelial sheet and the corneal epithelial sheets expressed significantly more MUC16 mRNA than the primary (uncultured) epithelial cells from oral mucosal tissue (Fig. 3) ($P = 0.023$ and $P = 0.008$, respectively, Mann–Whitney rank sum test). These findings were confirmed by immunohistochemical examination using an MUC16 antibody to the protein. MUC16 protein was localized in the apical cell layers of the cultivated oral sheets (Fig. 4A), and in the cultivated corneal epithelial sheet (Fig. 4B) and native corneal tissue (Fig. 4C). However, the oral mucosal tissue did not express MUC16 protein in any cell layers (Fig. 4D). This expression by the cultivated oral mucosal epithelial cells was observed in both the subconfluent (Fig. 4E) and confluent (Fig. 4F) stages.

4. Discussion

We showed that the expression patterns of MUC16 mRNA and protein levels differ between human oral mucosal tissue and cultivated oral mucosal epithelial sheets. The cultivated oral mucosal epithelial sheets expressed MUC16 on the apical surface of the stratified cells but MUC16 was much less expressed in the oral mucosal tissue. We previously reported that cultivated human oral mucosal epithelial sheets expressed MUC1, MUC4, and MUC16 mRNA, the expression patterns of which were the same as that in ocular surface epithelium (Hori et al., 2007). These new findings have extended the body of knowledge about the mechanism of oral mucosal sheet transplantation.

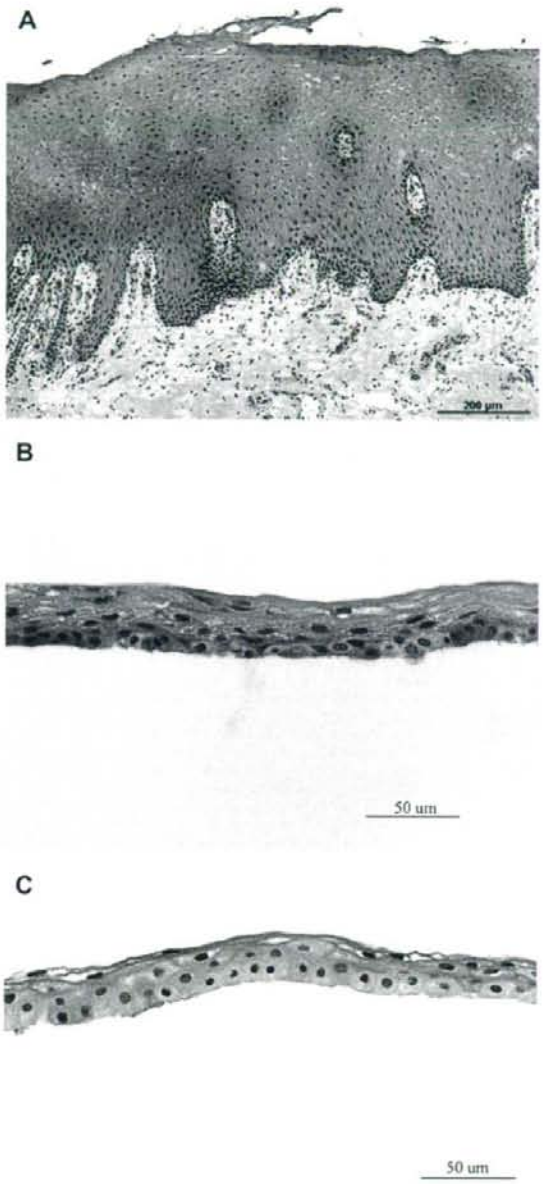

Fig. 1. Representative hematoxylin–eosin staining of the human oral mucosal tissue (A), and cultivated oral mucosal (B) and corneal (C) epithelial sheets. Native oral mucosal epithelial cells are stratified into 10–20 cell layers. Cultivated oral mucosal epithelial cells form three- to five-cell thick stratified sheets, as did the cultivated corneal epithelial sheets cultured under the same conditions.

MUC16 is thought to be the most important membrane-associated mucin on the ocular surface involved in the formation of a protective barrier on the epithelial cell surface (Argueso et al., 2006; Blalock et al., 2007). Inatomi et al. (2006) reported that oral mucosal epithelial cells survived on the ocular surface at least for 6 months after cultivated oral mucosal sheet transplantation.

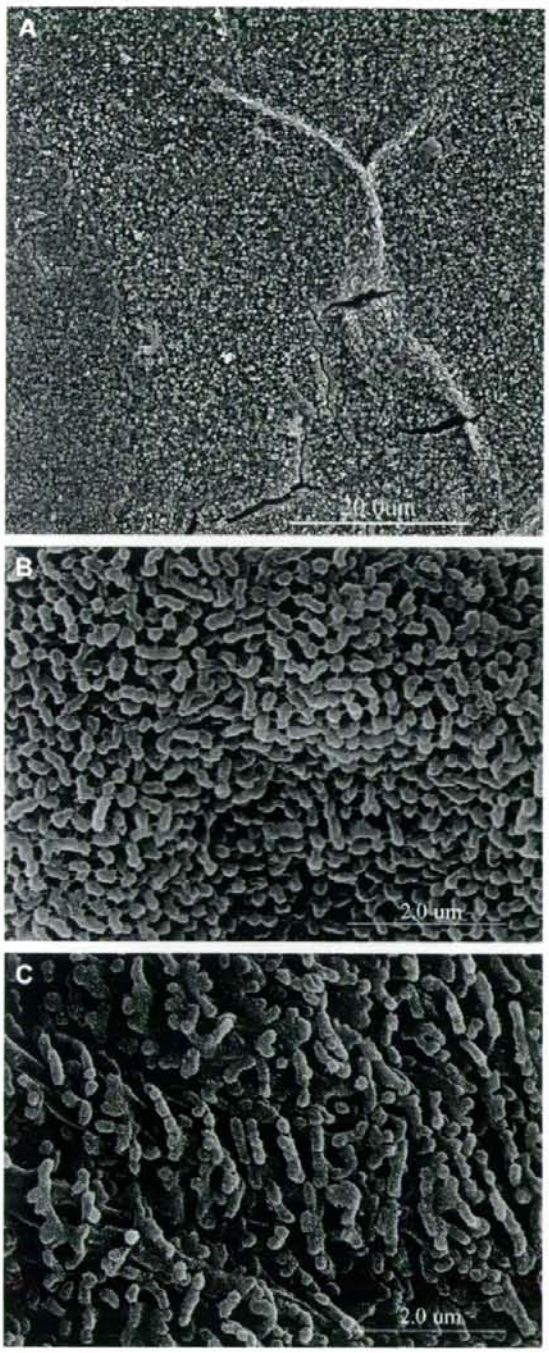

Fig. 2. Scanning electron micrographs of cultivated oral mucosal epithelial sheet (A and B) and excised oral mucosal epithelial tissue (C). The apical surface of the cultivated oral mucosal sheet is covered by numerous microvilli and microplicae, with morphology and dense similar to that of oral mucosal tissue.

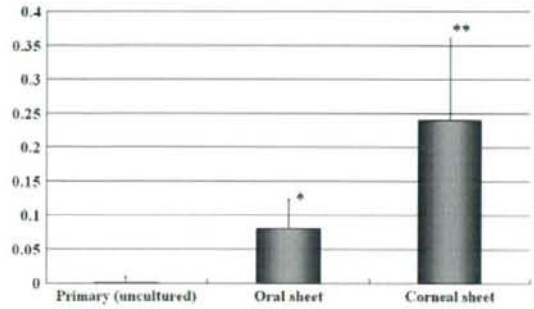

Fig. 3. Real-time PCR analysis of MUC16 mRNA expression in oral mucosal tissue, and cultivated oral mucosal and corneal epithelial sheet ($n = 3$). Each sample was assayed in triplicate. The cultivated oral and corneal epithelial sheet express significantly more MUC16 mRNA than the primary oral mucosal epithelial cells ($P = 0.023$ and $P = 0.008$, respectively, Mann–Whitney rank sum test). Error bars: S.E.M.

Therefore, MUC16 expressed on the apical surface of cultivated oral mucosal epithelia sheets may play important roles in stabilizing the ocular surface after transplantation of cultivated oral mucosal sheets, in that it prevents desiccation of the ocular surface and provides a barrier to penetration of pathogens.

It is unclear why the MUC16 expression differed between the cultivated oral mucosal epithelial sheets and the oral mucosal tissue. MUC16 is expressed on the tips of the microplicae of the ocular surface and is thought to be a major component of ocular surface glycocalyx, forming a protective barrier to the epithelial cell surface (Argueso et al., 2006; Blalock et al., 2007). Our SEM data demonstrated that the apical surface of the oral mucosal tissue was covered with numerous microvilli/microplicae with morphology and density similar to a cultivated oral mucosal epithelial sheet (Fig 2B and C). Blalock et al. (2007) reported similar findings, i.e., that the presence of microplicae on the surface of human corneal epithelial cells was unchanged in the MUC16 knockdown cells.

The limitation of the current study that may have affected interpretation of the results includes the fact that the oral mucosal tissue was surgically excised from the cheek. It is possible that the pre-treatment procedure during sample collection, i.e. sterilization of the oral cavity with topical povidone–iodine and/or local anesthesia with xylocaine could lead to shedding MUC16 from the surface of oral mucosal epithelial explants. Gipson et al. demonstrated that MUC16 is lost from the uterodome (pinopode) surface of the receptive human endometrium giving in vitro evidence that MUC16 is a barrier to trophoblast adherence (Gipson et al., 2008). Further investigations should be needed in these matters.

In the current study, we investigated MUC16 expression in oral mucosal epithelial cells harvested from normal healthy volunteers. Several abnormal conditions such as widespread erythema can be present in the mouths of patients with Stevens–Johnson syndrome (Abdollahi and Radfar, 2003). Additional investigations regarding the expression of membrane-associated mucins in patients with ocular surface disorders are needed to compare the expression patterns with those of healthy volunteers.

In summary, we reported that cultivated human oral mucosal epithelial sheets express the membrane-associated mucin MUC16 on the apical surface of the cells. We also showed that MUC16 expression differs from that in the oral mucosal tissue. We hypothesized that certain culture conditions may enhance induction of MUC16 expression in the cultivated oral mucosal epithelial cells or that certain conditions in the oral cavity may diminish its expression in the oral mucosal tissue. We believe that MUC16 expression in the cultivated oral mucosal sheets is an important hydrating

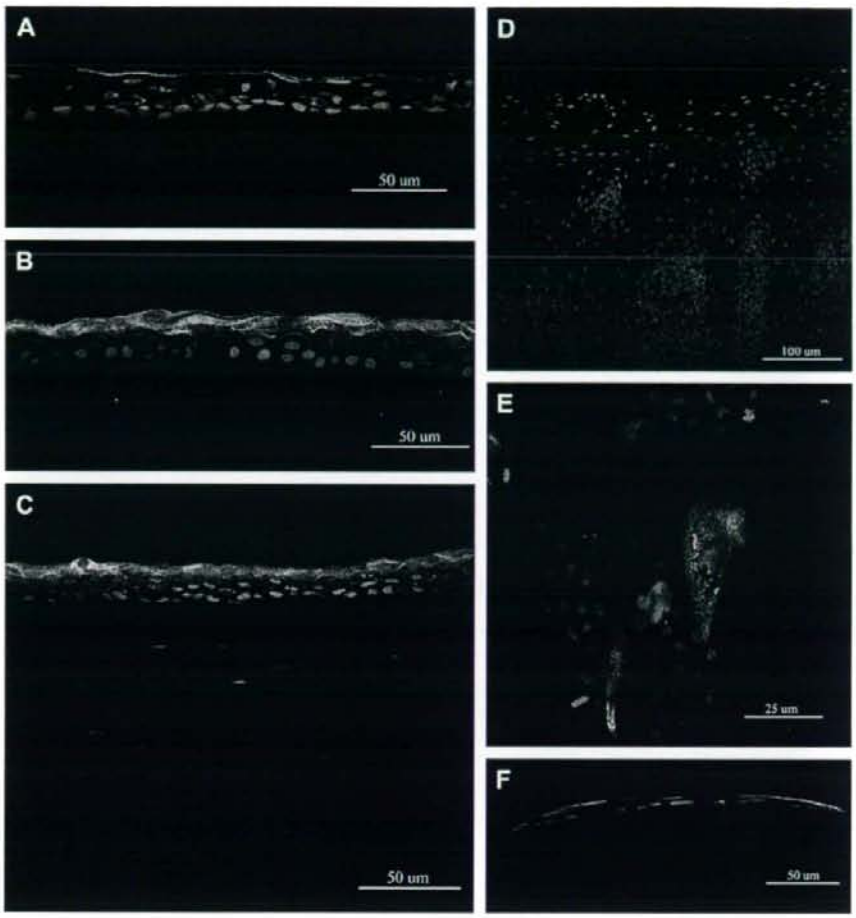

Fig. 4. Representative immunohistochemical staining for MUC16 antibody (OC125) in the cultivated oral (A) and corneal (B) epithelial sheets, native corneal (C) and oral mucosal (D) tissue, and subconfluent (E) and confluent (F) states of cultivated oral mucosal epithelial sheet. MUC16 protein is localized in the apical cell layers of the cultivated oral sheets (A) and the cultivated corneal epithelial sheets (B), and the native corneal tissue (C), but MUC16 protein is not expressed in any cell layers of the oral mucosal tissue (D). This expression by the cultivated oral mucosal epithelial cells also is observed in the subconfluent (E) and confluent (F) stages.

molecule that forms a protective barrier on the epithelial cell surface after sheet transplantation.

Acknowledgments

The authors thank Dr. Yoko Ogawa of Keio University for helpful advice regarding SEM. Supported by grant 18591920 from the Japanese Ministry of Education, Culture, Sports Science and Technology, and 2006 and 2007 the Osaka Eye Bank Society Research Grant to Y.H. The authors have no proprietary interest in any aspect of this report.

References

Abdollahi, M., Radfar, M., 2003. A review of drug-induced oral reactions. J. Contemp. Dent. Pract 4, 10–31.

Argueso, P., Balaram, M., Spurr-Michaud, S., Keutmann, H.T., Dana, M.R., Gipson, I.K., 2002. Decreased levels of the goblet cell mucin MUC5AC in tears of patients with Sjogren syndrome. Invest. Ophthalmol. Vis. Sci. 43, 1004–1011.

Argueso, P., Spurr-Michaud, S., Russo, C.L., Tisdale, A., Gipson, I.K., 2003. MUC16 mucin is expressed by the human ocular surface epithelia and carries the H185 carbohydrate epitope. Invest. Ophthalmol. Vis. Sci. 44, 2487–2495.

Argueso, P., Tisdale, A., Spurr-Michaud, S., Sumiyoshi, M., Gipson, I.K., 2006. Mucin characteristics of human corneal-limbal epithelial cells that exclude the rose bengal anionic dye. Invest. Ophthalmol. Vis. Sci. 47, 113–119.

Blalock, T.D., Spurr-Michaud, S.J., Tisdale, A.S., Heimer, S.R., Gilmore, M.S., Ramesh, V., Gipson, I.K., 2007. Functions of MUC16 in corneal epithelial cells. Invest. Ophthalmol. Vis. Sci. 48, 4509–4518.

Bobek, L.A., Tsai, H., Biesbrock, A.R., Levine, M.J., 1993. Molecular cloning, sequence, and specificity of expression of the gene encoding the low molecular weight human salivary mucin (MUC7). J. Biol. Chem. 268, 20563–20569.

Danjo, Y., Hazlett, L.D., Gipson, I.K., 2000. C57BL/6 mice lacking Muc1 show no ocular surface phenotype. Invest. Ophthalmol. Vis. Sci. 41, 4080–4084.

Fleiszig, S.M., Zaidi, T.S., Ramphal, R., Pier, G.B., 1994. Modulation of Pseudomonas aeruginosa adherence to the corneal surface by mucus. Infect. Immun. 62, 1799–1804.

Gipson, I.K., 2004. Distribution of mucins at the ocular surface. Exp. Eye Res. 78, 379–388.

Gipson, I.K., Argueso, P., 2003. Role of mucins in the function of the corneal and conjunctival epithelia. Int. Rev. Cytol. 231, 1–49.

Gipson, I.K., Spurr-Michaud, S., Argueso, P., Tisdale, A., Ng, T.F., Russo, C.L., 2003. Mucin gene expression in immortalized human corneal-limbal and conjunctival epithelial cell lines. Invest. Ophthalmol. Vis. Sci. 44, 2496–2506.

Gipson, I.K., Blalock, T., Tisdale, A., Spurr-Michaud, S., Allcorn, S., Stavreus-Evers, A., Gemzell, K., 2008. MUC16 is lost from the uterodome (pinopode) surface of the receptive human endometrium: in vitro evidence that MUC16 is a barrier to trophoblast adherence. Biol. Reprod. 78, 134–142.

Hattrup, C.L., Gendler, S.J., 2008. Structure and function of the cell surface (tethered) mucins. Annu. Rev. Physiol. 70, 431–457.

Hayashida, Y., Nishida, K., Yamato, M., Watanabe, K., Maeda, N., Watanabe, H., Kikuchi, A., Okano, T., Tano, Y., 2005. Ocular surface reconstruction using autologous rabbit oral mucosal epithelial sheets fabricated ex vivo on a temperature-responsive culture surface. Invest. Ophthalmol. Vis. Sci. 46, 1632–1639.

Hirose, M., Kwon, O.H., Yamato, M., Kikuchi, A., Okano, T., 2000. Creation of designed shape cell sheets that are noninvasively harvested and moved onto another surface. Biomacromolecules 1, 377–381.

Hori, Y., Spurr-Michaud, S., Russo, C.L., Argueso, P., Gipson, I.K., 2004. Differential regulation of membrane-associated mucins in the human ocular surface epithelium. Invest. Ophthalmol. Vis. Sci. 45, 114–122.

Hori, Y., Sugiyama, H., Soma, T., Nishida, K., 2007. Expression of membrane-associated mucins in cultivated human oral mucosal epithelial cells. Cornea 26, S65–S69.

Inatomi, T., Spurr-Michaud, S., Tisdale, A.S., Gipson, I.K., 1995. Human corneal and conjunctival epithelia express MUC1 mucin. Invest. Ophthalmol. Vis. Sci. 36, 1818–1827.

Inatomi, T., Spurr-Michaud, S., Tisdale, A.S., Zhan, Q., Feldman, S.T., Gipson, I.K., 1996. Expression of secretory mucin genes by human conjunctival epithelia. Invest. Ophthalmol. Vis. Sci. 37, 1684–1692.

Inatomi, T., Nakamura, T., Kojyo, M., Koizumi, N., Sotozono, C., Kinoshita, S., 2006. Ocular surface reconstruction with combination of cultivated autologous oral mucosal epithelial transplantation and penetrating keratoplasty. Am. J. Ophthalmol. 142, 757–764.

Jager, K., Wu, G., Sel, S., Garreis, F., Brauer, L., Paulsen, F.P., 2007. MUC16 in the lacrimal apparatus. Histochem. Cell Biol. 127, 433–438.

Jumblatt, M.M., McKenzie, R.W., Steele, P.S., Emberts, C.G., Jumblatt, J.E., 2003. MUC7 expression in the human lacrimal gland and conjunctiva. Cornea 22, 41–45.

Kenyon, K.R., Tseng, S.C., 1989. Limbal autograft transplantation for ocular surface disorders. Ophthalmology 96, 709–722. discussion 722–3.

Kinoshita, S., Adachi, W., Sotozono, C., Nishida, K., Yokoi, N., Quantock, A.J., Okubo, K., 2001. Characteristics of the human ocular surface epithelium. Prog. Retin. Eye Res. 20, 639–673.

Kutta, H., May, J., Jaehne, M., Munscher, A., Paulsen, F.P., 2006. Antimicrobial defence mechanisms of the human parotid duct. J. Anat. 208, 609–619.

Liu, B., Lague, J.R., Nunes, D.P., Toselli, P., Oppenheim, F.G., Soares, R.V., Troxler, R.F., Offner, G.D., 2002. Expression of membrane-associated mucins MUC1 and MUC4 in major human salivary glands. J. Histochem. Cytochem. 50, 811–820.

McKenzie, R.W., Jumblatt, J.E., Jumblatt, M.M., 2000. Quantification of MUC2 and MUC5AC transcripts in human conjunctiva. Invest. Ophthalmol. Vis. Sci. 41, 703–708.

Nakamura, T., Inatomi, T., Sotozono, C., Amemiya, T., Kanamura, N., Kinoshita, S., 2004. Transplantation of cultivated autologous oral mucosal epithelial cells in patients with severe ocular surface disorders. Br. J. Ophthalmol. 88, 1280–1284.

Nakamura, T., Inatomi, T., Cooper, L.J., Rigby, H., Fullwood, N.J., Kinoshita, S., 2007. Phenotypic investigation of human eyes with transplanted autologous cultivated oral mucosal epithelial sheets for severe ocular surface diseases. Ophthalmology 114, 1080–1088.

Nielsen, P.A., Bennett, E.P., Wandall, H.H., Therkildsen, M.H., Hannibal, J., Clausen, H., 1997. Identification of a major human high molecular weight salivary mucin (MG1) as tracheobronchial mucin MUC5B. Glycobiology 7, 413–419.

Nishida, K., Yamato, M., Hayashida, Y., Watanabe, K., Maeda, N., Watanabe, H., Yamamoto, K., Nagai, S., Kikuchi, A., Tano, Y., Okano, T., 2004a. Functional bioengineered corneal epithelial sheet grafts from corneal stem cells expanded ex vivo on a temperature-responsive cell culture surface. Transplantation 77, 379–385.

Nishida, K., Yamato, M., Hayashida, Y., Watanabe, K., Yamamoto, K., Adachi, E., Nagai, S., Kikuchi, A., Maeda, N., Watanabe, H., Okano, T., Tano, Y., 2004b. Corneal reconstruction with tissue-engineered cell sheets composed of autologous oral mucosal epithelium. N. Engl. J. Med. 351, 1187–1196.

O'Brien, T.J., Beard, J.B., Underwood, L.J., Shigemasa, K., 2002. The CA 125 gene: a newly discovered extension of the glycosylated N-terminal domain doubles the size of this extracellular superstructure. Tumour Biol. 23, 154–169.

Paulsen, F., Jager, K., Worlitzsch, D., Brauer, L., Schulze, U., Schafer, G., Sel, S., 2008. Regulation of MUC16 by inflammatory mediators in ocular surface epithelial cell lines. Ann. Anat. 190, 59–70.

Pflugfelder, S.C., Liu, Z., Monroy, D., Li, D.Q., Carvajal, M.E., Price-Schiavi, S.A., Idris, N., Solomon, A., Perez, A., Carraway, K.L., 2000. Detection of sialomucin complex (MUC4) in human ocular surface epithelium and tear fluid. Invest. Ophthalmol. Vis. Sci. 41, 1316–1326.

Sekiyama, E., Nakamura, T., Kawasaki, S., Sogabe, H., Kinoshita, S., 2006. Different expression of angiogenesis-related factors between human cultivated corneal and oral epithelial sheets. Exp. Eye Res. 83, 741–746.

Sengupta, A., Valdramidou, D., Huntley, S., Hicks, S.J., Carrington, S.D., Corfield, A.P., 2001. Distribution of MUC1 in the normal human oral cavity is localized to the ducts of minor salivary glands. Arch. Oral Biol. 46, 529–538.

Tan, D.T., Ficker, L.A., Buckley, R.J., 1996. Limbal transplantation. Ophthalmology 103, 29–36.

Thoft, R.A., 1984. Keratoepithelioplasty. Am. J. Ophthalmol. 97, 1–6.

Tseng, S.C., 1989. Concept and application of limbal stem cells. Eye 3 (Pt 2), 141–157.

Tsubota, K., Satake, Y., Ohyama, M., Toda, I., Takano, Y., Ono, M., Shinozaki, N., Shimazaki, J., 1996. Surgical reconstruction of the ocular surface in advanced ocular cicatricial pemphigoid and Stevens-Johnson syndrome. Am. J. Ophthalmol. 122, 38–52.

Yin, B.W., Lloyd, K.O., 2001. Molecular cloning of the CA125 ovarian cancer antigen: identification as a new mucin, MUC16. J. Biol. Chem. 276, 27371–27375.

PI3K/Akt signaling as a key regulatory pathway for chondrocyte terminal differentiation

Keisuke Kita[1,2], Tohru Kimura[1,*], Norimasa Nakamura[2], Hideki Yoshikawa[2] and Toru Nakano[1,3,*]

[1]*Department of Pathology, and*
[2]*Department of Orthopedics, Graduate School of Medicine, and*
[3]*Graduate School of Frontier Biosciences, Osaka University, 2-2 Yamada-oka, Suita, Osaka 565-0871, Japan*

Chondrogenesis is a well-coordinated multi-step differentiation process in which resting chondrocytes produce terminally differentiated hypertrophic chondrocytes through a proliferative stage. Here we show that phosphoinositide-3 kinase (PI3K) and its major downstream molecule, Akt, a serine–threonine kinase, play pivotal roles in this process. Akt signaling was activated in resting and proliferative chondrocytes but was reduced during terminal differentiation. We adopted two chondrocyte differentiation systems to investigate the roles of PI3K/Akt signaling in chondrogenesis. First, we employed an embryonic forelimb organ culture of transgenic mice expressing an Akt-Mer (a ligand-binding domain of a mutated estrogen receptor) fusion protein whose kinase activity was conditionally activated by treatment with 4-hydroxytamoxifen (4OHT). Activation of Akt signaling in embryonic chondrogenesis enhanced chondrocyte proliferation and inhibited hypertrophic differentiation, presumably due to the suppressed expression of Runx2, a transcription factor critical for chondrocyte terminal differentiation. Conversely, inhibition of PI3K by its inhibitor accelerated terminal hypertrophic differentiation, resulting in a shorter bone. Essentially the same results were obtained in a second line of experiments using human synovial stromal cells (hSSCs), which are mesenchymal progenitor cells isolated from adult joints. These findings demonstrate that PI3K/Akt signaling is a key regulator in terminal chondrocyte differentiation in both embryonic and adult chondrogenesis.

Introduction

In vertebrates, there are two patterns of bone development: endochondral and intramembranous bone formation (Kronenberg 2003; Goldring *et al.* 2006). The former is initiated when mesenchymal cells condense and then differentiate into chondrocytes. The production and secretion of aggrecan, a matrix that is rich in proteoglycan and type II collagen, from chondrocytes is necessary to form cartilage. As cartilage enlarges, resting chondrocytes at both ends of bone rudiments differentiate into proliferative chondrocytes (Fig. 1A). After cell division ceases in proliferative chondrocytes, they enter terminal differentiation. The resulting hypertrophic chondrocytes mineralize their surrounding matrix, secrete type X collagen, and attract chondroclasts and osteoclasts through conducting vessels. Finally, the hypertrophic chondrocytes undergo apoptotic cell death, and the remaining matrix provides a scaffold for osteoblasts to form cancellous bone.

Terminal chondrocyte differentiation is regulated by a transcription factor, Runx2. The expression of Runx2 dramatically increases in prehypertrophic chondrocytes and is maintained during hypertrophy (Enomoto *et al.* 2000). Hypertrophic chondrocyte genes such as *Col10a1* and *MMP-13* are under the control of Runx2 (Jimenez *et al.* 1999; Zheng *et al.* 2003). Runx2-deficient mice exhibit slower chondrocyte differentiation and lack of osteoblast differentiation (Komori *et al.* 1997; Otto *et al.* 1997; Inada *et al.* 1999; Kim *et al.* 1999). Furthermore, the enforced expression of *Runx2* induces precocious chondrocyte maturation, whereas the dominant negative form of *Runx2* inhibits chondrocyte terminal differentiation (Enomoto *et al.* 2000; Ueta *et al.* 2001). In light of

Communicated by: Tetsuya Taga
**Correspondence*: tkimura@patho.med.osaka-u.ac.jp; tnakano@patho.med.osaka-u.ac.jp

DOI: 10.1111/j.1365-2443.2008.01209.x

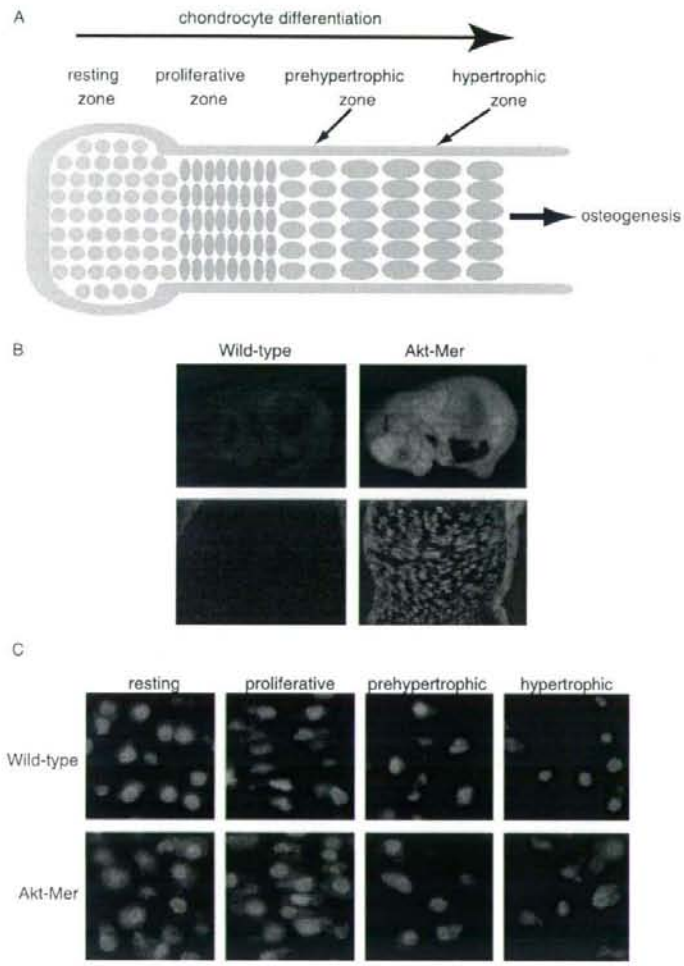

Figure 1 Down-regulation of Akt signaling in the terminal differentiation of chondrocytes. (A) Scheme of chondrogenesis in mouse embryonic forelimbs. Resting chondrocytes are differentiated from mesenchymal precursor cells during endochondral bone development. Chondrocytes undergo multi-step differentiation processes to produce the terminally differentiated hypertrophic chondrocytes *via* proliferative and pre-hypertrophic phases. (B) Expression of EGFP in Akt-Mer transgenic mice. Akt-Mer transgenic mice at E14.5 showed strong EGFP fluorescence in their whole bodies and in cartilage chondrocytes. (C) Akt signaling activation in chondrogenesis. The forelimbs of wild-type and Akt-Mer transgenic mice were cultured in 4OHT and immunodetected with anti-phospho (Ser473)-Akt antibody (red). In wild-type mice, strong phospho-Akt signals were detected in resting and proliferative chondrocytes, but the signals gradually decreased in pre-hypertrophic and hypertrophic chondrocytes (upper panels). In contrast, significantly stronger signals were observed in all of the differentiation stages of chondrocytes of Akt-Mer transgenic mice (lower panels). Nuclei were counterstained with DAPI (blue).

these observations, it has been proposed that Runx2 is a critical transcriptional regulator for terminal chondrocyte differentiation. Meanwhile, the parathyroid hormone-related protein (PTHrP)/Indian hedgehog (Ihh) feedback loop has also been reported to control differentiation from proliferative to hypertrophic chondrocytes (Vortkamp *et al.* 1996). However, other than the roles of Runx2 and the PTHrP/Ihh feedback loop, the molecular basis of the control of chondrocyte terminal differentiation remains elusive.

Mesenchymal progenitor cells are cells that differentiate into various tissues, such as bone, cartilage, and adipose tissues (Pittenger *et al.* 1999). Although mesenchymal progenitor cells were first identified in bone marrow, they have also been identified in adipose tissue (Zuk *et al.* 2001), muscle (Jankowski *et al.* 2002), tendon (Salingcarnboriboon *et al.* 2003), and synovium (De Bari *et al.* 2001). Synovium-derived stromal cells (SSCs) have a higher chondrogenic potency than mesenchymal progenitor cells derived from bone marrow and adipose

tissue (Sakaguchi *et al.* 2005). In fact, human SSCs (hSSCs) migrate into articular cartilage lesions, where they differentiate into chondrocyte progenitor cells (Hunziker & Rosenberg 1996). Considering that a sufficient amount of hSSCs can easily be obtained from knee joints without donor-site morbidity (Tateishi *et al.* 2007), hSSCs could be a promising source of cell-based cartilage repair.

Phosphoinositide-3 kinase (PI3K)/Akt signaling may regulate cell proliferation, growth, migration, death, adhesion, and tumorigenesis in various cell lineages (Cantley 2002). Akt, a serine–threonine kinase, is activated by phosphatidylinositol (3,4,5)-triphosphate (PtdIns(3,4,5)P3), which is generated from PtdIns(4,5)P2 by PI3K (Brazil *et al.* 2004). In this study, we examined the function of PI3K/Akt signaling in chondrogenesis (during endochondral bone formation) and chondrogenic differentiation in hSSCs. Activation of Akt inhibited the terminal differentiation of proliferative chondrocytes into hypertrophic chondrocytes in two independent experimental systems of chondrogenesis. In contrast, the transition from proliferation to hypertrophy was promoted by the inhibition of PI3K/Akt signaling. Thus, our results offer novel insights into the function of PI3K/Akt signaling in chondrocyte differentiation.

Results

Down-regulation of Akt activation in terminally differentiated chondrocytes

We first examined the effects of Akt signaling activation on chondrocyte differentiation. We used transgenic mice expressing an Akt-Mer fusion protein (Murayama *et al.* 2007), a synthetic protein composed of a myristoylated constitutively active form of Akt and the ligand-binding domain of a mutant estrogen receptor (Mer) (Kohn *et al.* 1998). The kinase activity of Akt-Mer can be conditionally controlled because it is inactivated in the absence of 4-hydroxytamoxifen (4OHT) and activated in the presence of 4OHT (Watanabe *et al.* 2006). As Mer is insensitive to endogenous estrogen (Littlewood *et al.* 1995), Akt-Mer constitutes a valuable system to control this signal at the organ and tissue levels.

Because the Akt-Mer cDNA is ligated to a cDNA encoding an internal ribosomal entry site-enhanced green fluorescent protein (IRES-EGFP), the expression of Akt-Mer can be monitored using EGFP fluorescence. Akt-Mer transgenic mice at embryonic day 14.5 (E14.5) showed strong EGFP fluorescence in cartilage rudiments (Fig. 1B). Immunohistochemistry using an anti-phosphorylated Akt antibody revealed strong signals in the resting and proliferative chondrocytes of wild-type cartilage rudiments (Fig. 1C). As differentiation proceeded, the signals gradually decreased, and only weak signals could be detected in the hypertrophic zone. In contrast, significantly stronger signals were observed in all of the chondrocyte differentiation stages in Akt-Mer transgenic mice treated with 4OHT (Fig. 1C).

Inhibition of chondrocyte terminal differentiation by Akt

To investigate the role of PI3K/Akt signaling in chondrocyte differentiation, we used a mouse embryonic forelimb explant culture system. This system allowed us to cultivate cartilage rudiments free of the effects of systemic hormonal or neuronal stimulation that could influence cartilage metabolism during the endochondral ossification process, and to analyze the effects of any cytokines or chemicals. Radii were isolated from each E14.5 Akt-Mer transgenic mouse embryo and a wild-type littermate control and cultured for 5 days in 4OHT. There were no detectable differences between the groups of mice at the beginning of the culture (Fig. 2A). During the culture, however, bone rudiment elongation was significantly enhanced in Akt-Mer transgenic mice (Fig. 2A,B). At day 5 of the culture, two opaque zones that corresponded macroscopically to hypertrophic zones became apparent on both sides of the ossificated zones in wild-type rudiments (arrowheads in Fig. 2A). In contrast, no opaque zones were observed in the transgenic rudiments, showing that hypertrophic differentiation was impaired in 4OHT-treated transgenic chondrocytes.

Morphological analysis of sections stained with Alcian blue revealed that the proliferative zone was elongated; only a few hypertrophic chondrocytes were detectable in 4OHT-treated transgenic bone rudiments (Fig. 2C). These phenotypes were not observed in untreated transgenic rudiments (data not shown). Furthermore, Akt activation suppressed the expression of hypertrophic chondrocyte markers such as Runx2 and type X collagen (Fig. 2D,E). These results indicate that Akt activation induced the expansion of proliferative chondrocytes and inhibited terminal differentiation into hypertrophic chondrocytes.

Promotion of chondrocyte terminal differentiation by PI3K signaling inhibition

Akt signaling was activated in proliferative chondrocytes but down-modulated during the course of terminal differentiation (Fig. 1C). To determine the physiological relevance of endogenous PI3K/Akt signaling in chondrogenesis, we cultured wild-type forelimbs with a

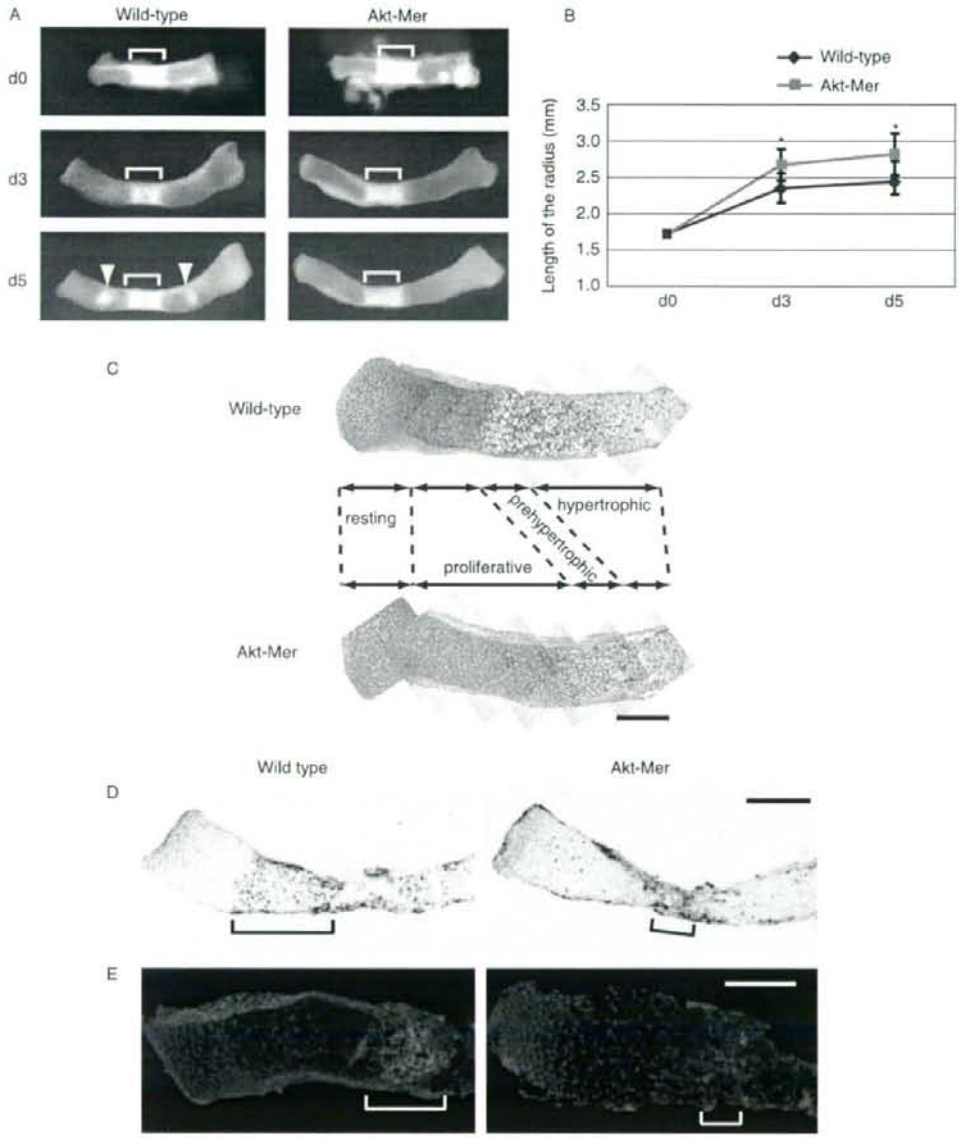

PI3K inhibitor, LY294002, or the vehicle DMSO. Bone rudiment elongation was significantly suppressed by treatment with LY294002 in a dose-dependent manner (Fig. 3A). Macroscopic analysis showed that the opaque zones corresponding to hypertrophic zones were more prominent in LY294002-treated bones than in DMSO-treated bones (Fig. 3B). Immunohistochemical analysis revealed that the deposition of type X collagen increased in rudiments treated with LY294002 (Fig. 3C). These results indicate that terminal chondrocyte differentiation was accelerated by the inhibition of PI3K signaling. These results, together with those of the Akt-Mer transgenic mice studies, suggest that PI3K/Akt signaling regulates the transition from proliferative to hypertrophic chondrocytes.

Inhibition of chondrocyte terminal differentiation of human SSCs by activation of Akt signaling

In contrast to embryonic chondrogenesis during endochondral bone formation, chondrogenesis in adult tissues may originate in mesenchymal progenitor cells. To assess the function of PI3K/Akt in adult chondrogenesis, hSSCs were infected with lentivirus expressing Akt-Mer and differentiated into chondrocytes through a cartilaginous pellet culture procedure (Johnstone *et al.* 1998). The Akt-Mer-transducted hSSCs and control hSSCs were aggregated by centrifugation and cultured for 21 days in TGF-β1. The pellets were significantly larger in 4OHT-treated Akt-Mer-transduced hSSCs than the others (Fig. 4A,B). The Akt-Mer-transduced pellets were larger than those from control hSSCs even in the absence of 4OHT, presumably due to the weak and leaky activation of Akt-Mer protein even in the absence of 4OHT, as evidenced by anti-phospho-Akt staining (Fig. 4A).

The area stained with Alcian blue was significantly enlarged by Akt activation (upper panels of Fig. 4C). The 4OHT-treated Akt-Mer-transducted cells had round chondrocytic morphology, whereas the others were reminiscent of a fibroblastic phenotype (middle and bottom panels of Fig. 4C). Cartilaginous lacuna-like cavities were also induced by Akt activation (middle and bottom panels of Fig. 4C), and glycosaminoglycan (GAG) levels were higher in Akt-activated pellets (Fig. 4D). Semi-quantitative RT-PCR analysis revealed no obvious differences in the mRNA levels of the early chondrogenic markers *Sox9*, *Col2a1*, and *Aggrecan* in Akt-activated cells and the other cells (Fig. 4E). However, the expression of the terminal chondrogenic marker genes *Runx2* and *Col10a1* in Akt-activated pellets was lower and undetectable, respectively (Fig. 4E). These results show that the hyperactivation of Akt signaling inhibited terminal differentiation in chondrogenesis from multi-potent hSSCs, which is essentially the same result as that obtained in the previous analysis of Akt-Mer transgenic mice.

Next, we added the PI3K inhibitor LY294002 to a pellet culture of parental hSSCs. The pellets were significantly smaller (Fig. 5A,B) and the area stained in Alcian blue was lower in pellets treated with LY294002 (Fig. 5C). Decreased pellet size and inhibited chondrocytic differentiation were similarly observed in cultures treated with the Akt inhibitor NL-71–101 (Fig. S1 in Supplementary Material). RT-PCR analysis showed that the inhibition of PI3K decreased the expression of the early chondrocyte markers *Sox9*, *Col2a1*, and *Aggrecan* but increased the expression of the terminal differentiation markers *Runx2* and *Col10a1* (Fig. 5D). Thus, endogenous activation of PI3K/Akt negatively regulates the transition from the proliferative to the hypertrophic stage, not only in embryonic chondrogenesis but also in adult chondrogenesis in hSSCs.

Figure 2 Promotion of bone-rudiment elongation and inhibition of terminal differentiation of embryonic chondrocytes by Akt signaling. (A) Macroscopic photos of cultured bone rudiments. Bone rudiments of E14.5 wild-type and Akt-Mer transgenic mice were cultured in 5 μM 4OHT. No significant differences were observed between the radii of the two groups of mice at day 0. At day 3 of the culture, bone rudiment elongation began to be more pronounced in Akt-Mer transgenic mice. At day 5, two opaque zones corresponding to hypertrophic zones became visible in wild-type mice but not in Akt-Mer transgenic mice (arrowheads in the lower panels). The ossification zones are marked with brackets. (B) Lengths of bone rudiments in culture. Bones were significantly longer in the 4OHT-treated Akt-Mer transgenic mice at days 3 and 5 of the culture (*$P < 0.01$ by Student's *t*-test). Data are shown as mean ± SD of six samples. (C) Histology of radius sections stained with Alcian blue. In Akt-Mer transgenic mice, the proliferation zone was elongated but the numbers of pre-hypertrophic and hypertrophic chondrocytes were dramatically lower. The nuclei were counterstained with Kernechtrot. Bar = 0.2 mm. (D) Expression of the *Runx2* mRNA. *Runx2* expression was examined by *in-situ* hybridization using an antisense *Runx2* probe. *Runx2*-positive cells were detected in pre-hypertrophic and hypertrophic zones of wild-type mice, but not in Akt-Mer transgenic mice. Bars = 0.4 mm. (E) Immunostaining with an antibody against Type X collagen. Type X collagen was deposited in the hypertrophic zone of wild-type mice but not in the bone rudiments of Akt-Mer transgenic mice. Bars = 0.2 mm.

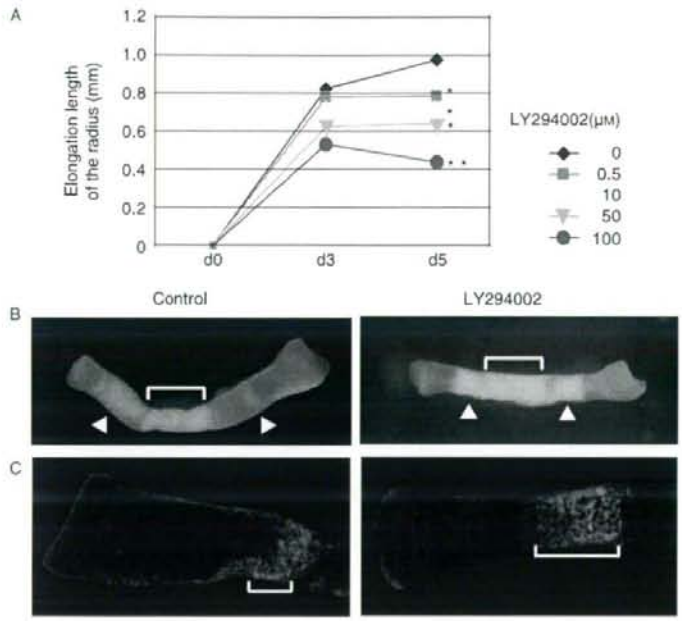

Figure 3 Promotion of chondrocyte differentiation by a PI3K inhibitor. (A) Effects of a PI3K inhibitor on bone-rudiment elongation. Bone rudiments of wild-type mice at E14.5 were cultured for 5 days in various concentrations of LY294002. Bone-rudiment elongation was suppressed by LY294002 treatment in a dose-dependent manner (*$P < 0.05$, **$P < 0.01$ by Student's *t*-test). Means ± SD of six samples are as follows; 0.82 ± 0.04 (0 μM), 0.77 ± 0.05 (0.5 μM), 0.71 ± 0.03 (10 μM), 0.62 ± 0.11 (50 μM), 0.53 ± 0.02 (100 μM) for day 3; 0.96 ± 0.07 (0 μM), 0.78 ± 0.04 (0.5 μM), 0.69 ± 0.02 (10 μM), 0.63 ± 0.05 (50 μM), 0.43 ± 0.07 (100 μM) for day 5. (B) Macroscopic photographs of bone rudiments cultured in PI3K inhibitor. Bone rudiments were cultured in 1 μM LY294002 or DMSO. The opaque zones corresponding to hypertrophic zones were more prominent in LY294002-treated wild-type bones (arrowheads). The ossification zones are marked with brackets. (C) Immunostaining with an antibody against Type X collagen. Type X collagen deposition increased in the hypertrophic zones of bone rudiments treated with LY294002. Bars = 0.2 mm.

Figure 4 Effects of Akt activation on chondrogenic differentiation in hSSCs. (A) Chondrogenic differentiation of Akt-Mer-transducted hSSCs. hSSCs were infected with Akt-Mer-expressing lentivirus or control lentivirus. Chondrogenic differentiation was subsequently induced using a pellet procedure as described in the text. The cultures were incubated for 21 days in the presence or absence of 4OHT. Pellet sections were stained with anti-phospho-Akt antibody (lower panels). Strong phospho-Akt signals were observed in Akt-Mer-transduced hSSCs cultured in 4OHT. Weak and leaky phospho-Akt signals were also detected in Akt-Mer-transduced pellets cultured without 4OHT. (B) Pellet size. The 4OHT-treated Akt-Mer-transduced pellets were significantly larger than the controls (*$P < 0.01$ by Student's *t*-test). Even without 4OHT treatment, the Akt-Mer-transduced pellets were significantly larger than the control virus-transduced pellets (**$P < 0.05$ by Student's *t*-test). The data shown are means ± SD of nine samples. (C) Sections stained with Alcian blue. The stained areas were enlarged in 4OHT-treated Akt-Mer-transduced pellets (upper panels; bar, 500 μm), and their cells were larger and had a round chondrocytic morphology and cartilaginous lacuna-like cavities. The cells of the other pellets had a fibroblastic phenotype (middle panels; bar, 50 μm; lower panels; bar, 7.5 μm). Nuclei were counterstained with Kernechtrot. (D) GAG levels in pellets. The 4OHT-treated Akt-Mer-transduced pellets produced higher amounts of GAG than control pellets (**$P < 0.05$ by Student's *t*-test). n.s., not significantly different. The data shown are means ± SD of three samples. (E) Semi-quantitative RT-PCR analysis. Akt activation did not affect the expression of the early chondrogenic markers *Sox9*, *Col2a1*, or *Aggrecan*, but suppressed the expression of the terminal chondrogenic markers *Runx2* and *Col10a1*.

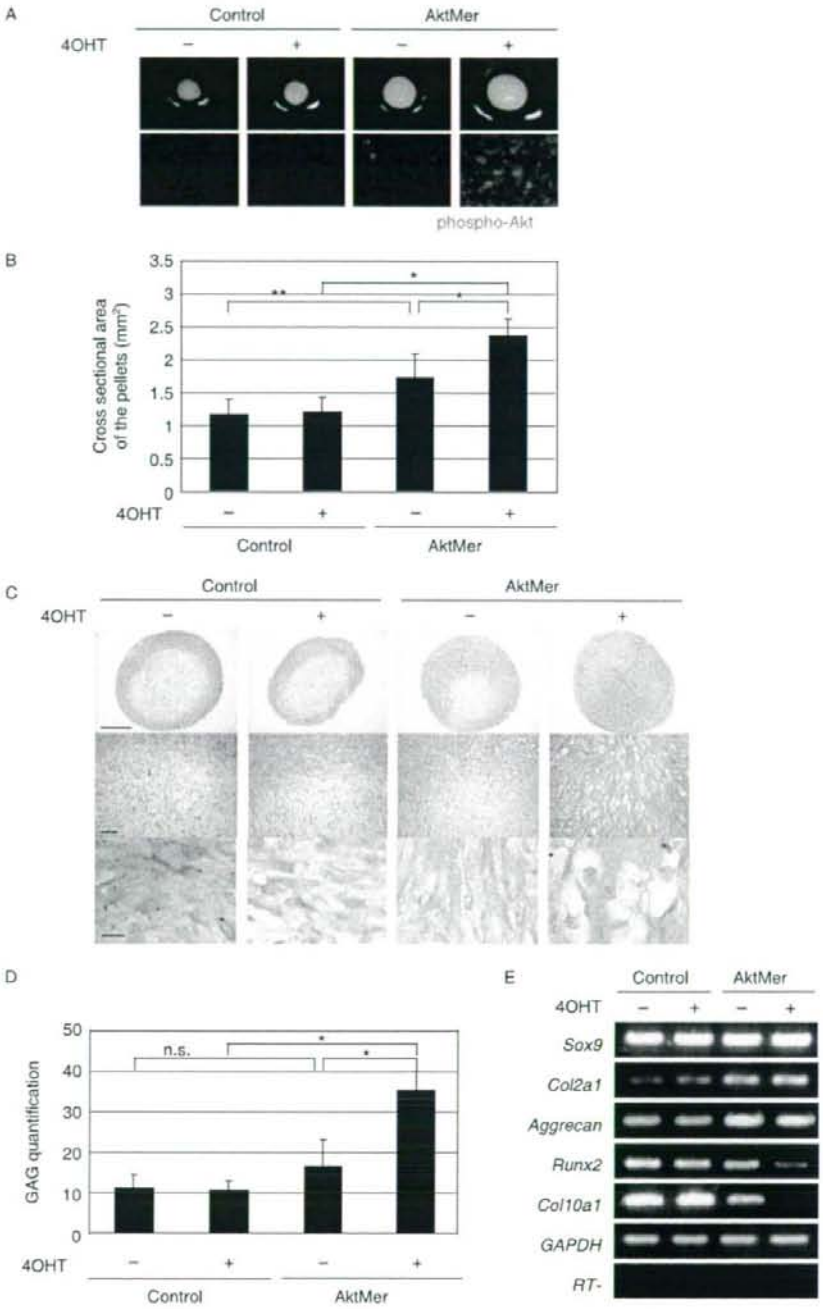

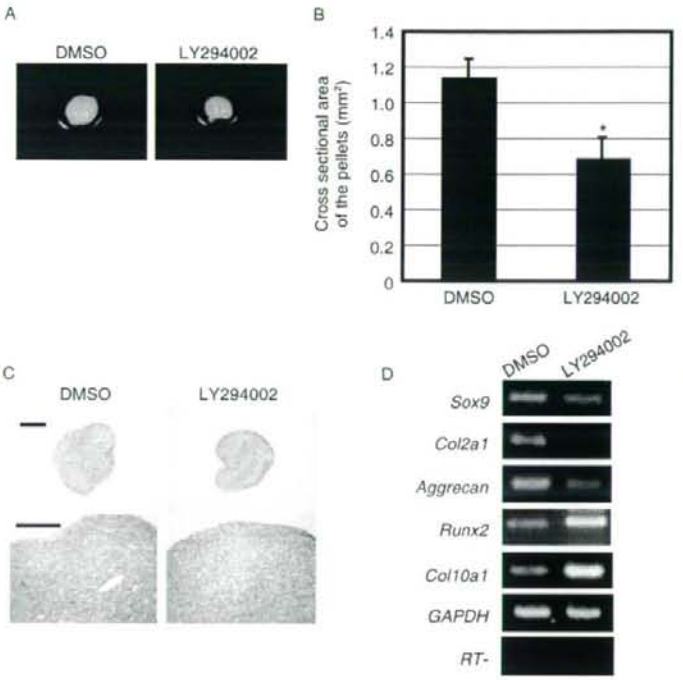

Figure 5 Promotion of terminal differentiation of chondrocytes in hSSCs using a PI3K inhibitor. (A) Pellets induced by PI3K inhibition. Chondrogenic differentiation was induced in hSSCs using a pellet procedure. At day 7 of the culture, 1 μM LY294002 or DMSO was added. The pellet cultures were then incubated for additional 14 days. (B) Pellet size. LY294002-treated pellets were significantly smaller than DMSO-treated controls ($^*P < 0.01$ by Student's *t*-test). The data shown are means ± SD of three samples. (C) Sections stained with Alcian blue. Stained areas were smaller in LY294002-treated pellets (upper panels, bar, 500 μm; lower panels, bar, 200 μm). Nuclei were counterstained with Kernechtrot. (D) Semi-quantitative RT-PCR analysis. Akt activation decreased the expression of the early chondrogenic markers *Sox9*, *Col2a1*, and *Aggrecan*, but enhanced the expression of the terminal chondrogenic markers *Runx2* and *Col10a1*.

Discussion

We have identified a novel function of PI3K/Akt signaling in chondrogenesis using two experimental systems: an *ex vivo* mouse embryonic forelimb culture and a system for the *in vitro* differentiation of human mesenchymal progenitor cells, hSSCs. In both analyses, Akt signaling activation induced the expansion of proliferative chondrocytes and inhibited terminal differentiation into hypertrophic chondrocytes. In contrast, inhibition of PI3K/Akt signaling accelerated terminal differentiation. These findings clearly demonstrate that terminal differentiation is negatively regulated by PI3K/Akt signaling in embryonic and adult chondrogenesis.

Several studies have reported that PI3K/Akt signaling exhibits pleiotropic functions in chondrogenesis. Analyses using prechondrogenic ATDC5 cells have shown that PI3K/Akt signaling promotes the differentiation of chondrocyte precursors into early-stage chondrocytes. A constitutively active form of Akt accelerates the insulin-dependent chondrogenic differentiation of ATDC5 cells (Hidaka *et al.* 2001). Conversely, PI3K inhibitor attenuates the expression of the early chondrocyte differentiation marker *Col2a1* and the production of proteoglycan in ATDC5 cells (Fujita *et al.* 2004b). Meanwhile, PI3K/Akt signaling is required for the proliferation of chondrocyte cell lines and the production of sulfated GAG in human primary articular chondrocytes (Oh & Chun 2003; Starkman *et al.* 2005; Priore *et al.* 2006; Qureshi *et al.* 2007). Our results are also in accordance with the notion that proliferation and cartilage matrix synthesis are augmented by PI3K/Akt signaling during the proliferative differentiation stage. Thus, PI3K/Akt promotes chondrogenic commitment and preserves the chondrogenic phenotype and function in the early differentiation stages.

PI3K/Akt signaling may also promote terminal chondrocyte differentiation in cooperation with Runx2 (Fujita *et al.* 2004a). Although the overexpression of Runx2 induces *Col10a1* expression in ATDC5 cells, this *Col10a1* induction is completely abrogated by the expression of a dominant-negative Akt. Furthermore, the levels of Akt and the PI3K subunits p85 and p110β are upregulated by Runx2 overexpression, whereas PI3K/Akt signaling enhances the DNA-binding ability of Runx2. These observations collectively suggest that PI3K/Akt signaling and Runx2 constitute a positive feedback loop to accomplish terminal differentiation in

Runx2-expressing hypertrophic chondrocytes. However, the role of PI3K/Akt signaling in the transition from the proliferative stage to terminal differentiation remained unclear, because hypertrophic differentiation was artificially induced by overexpressing Runx2 in the study of Fujita *et al.* (Fujita *et al.* 2004a).

To circumvent this problem, we used a forelimb organ culture in which chondrogenesis transitions to hypertrophy as it does *in vivo* (Serra *et al.* 1999). Combining this organ culture and a conditional Akt activation system (Murayama *et al.* 2007) provided compelling evidence that PI3K/Akt signaling inhibits the transition from proliferative to hypertrophic differentiation during endochondral ossification. In addition, we showed that PI3K/Akt signaling activation causes essentially the same phenomenon in chondrogenic differentiation in hSSCs. These results, together with those of Fujita (Fujita *et al.* 2004a), suggest that PI3K/Akt signaling exerts completely opposite influences on two aspects of terminal differentiation. Namely, it inhibits the transition from the proliferative stage to terminal differentiation, but once chondrocytes enter into the hypertrophic differentiation stage, it drives terminal differentiation to completion.

Hypoxia occurs in the interior of cartilaginous tissues during endochondral bone formation (Schipani *et al.* 2001). Culturing embryonic forelimbs and mesenchymal C3H10T1/2 cells under low oxygen levels leads to phenotypes that are similar to those induced by Akt activation (Hirao *et al.* 2006). Hypoxic treatment promotes chondrocytic commitment, increases cartilaginous matrix synthesis, and suppresses terminal chondrocyte differentiation. Thus, the transition to terminal differentiation is regulated by at least two extracellular environmental factors: growth factors and oxygen supply.

The hypoxia-induced inhibition of terminal differentiation is presumably caused by reduced *Runx2* expression, which could result from the suppression of Smad signaling and the activation of histone deacetylase 4 (HDAC4) (Hirao *et al.* 2006). We demonstrated that *Runx2* expression is decreased by Akt activation but increased by PI3K inhibition, which raises the possibility that *Runx2* is repressed at the transcriptional level by PI3K/Akt signaling. Because hypoxia-inducible factor 1 (HIF-1) is a transcription factor that is activated by both hypoxia and PI3K/Akt signaling (Bardos & Ashcroft 2004), it is possible that HIF-1 is involved in the regulation of *Runx2* in chondrogenesis. Alternatively, other downstream Akt transcription factors such as FOXO might play a role. Future studies should resolve the regulation of *Runx2* expression by PI3K/Akt signaling and hypoxia.

Cellular differentiation in various stem-cell systems is controlled by PI3K/Akt signaling. For instance, the pluripotent differentiation capacities of embryonic stem (ES) cells are prohibited by PI3K/Akt signaling activation (Paling *et al.* 2004; Ivanova *et al.* 2006; Watanabe *et al.* 2006). Enhancing PI3K/Akt activation causes the dedifferentiation of primordial germ cells into pluripotent embryonic germ (EG) cells *in vitro* and into testicular teratoma *in vivo* (Kimura *et al.* 2003, 2008). In addition, PI3K/Akt activation induces the expansion of stem/progenitor cell populations in epithelial stem cell systems (He *et al.* 2007; Murayama *et al.* 2007). Because these phenomena induced by PI3K/Akt signaling activation are accompanied by enhanced proliferation, it is likely that PI3K/Akt signaling inhibits cellular differentiation *via* mitotic activation in these stem-cell systems. Our results suggest that this is also the case with chondrogenesis, because PI3K/Akt signaling activation expanded proliferative chondrocytes but inhibited the differentiation into mitotically quiescent terminally differentiated cells.

In conclusion, we provide evidence that each step of chondrogenesis is regulated both positively and negatively by PI3K/Akt signaling, depending on the differentiation stage of the chondrocytes. Even if PI3K/Akt signaling is overactivated, this mechanism could prevent the exhaustion of immature precursors and the overproduction of terminally differentiated cells. Conversely, when this signaling is down-modulated, the mechanism could ensure that precursors enter into terminal differentiation. This kind of Yin Yang regulation may serve as a safeguard mechanism to the vulnerabilities inherent to unidirectional differentiation systems.

Experimental procedures

Organ culture of embryonic limb explants

Male Akt-Mer transgenic mice were crossed with female BDF1 mice (Charles River, Osaka, Japan) (Murayama *et al.* 2007). The forelimbs of E14.5 embryos of Akt-Mer transgenic mice and wild-type littermates were stripped of their skin and muscle and the radii removed. The radii were cultured for 5 days at 37 °C in a humidified 5% CO_2 incubator in 24-well plates in alpha-MEM (Gibco BRL, Rockville, MD) supplemented with 0.05 ng/mL ascorbic acid, 0.3 mg/mL L-glutamine, 1% penicillin/streptomycin, 1 mM β-glycerophosphate, and 0.2% bovine serum albumin (Serra *et al.* 1999). Cultures of Akt-Mer transgenic and wild-type rudiments were supplemented with 5 μM 4-hyroxytamoxifen (4OHT; Sigma, St Louis, MO) or 0.5–100 μM LY294002 (Calbiochem, San Diego, CA). Photographs of cultured bones were taken with a Leica MZ 16 F (Leica Microsystems, Wetzlar, Germany), and bone length was measured using Leica IM500 software.